Cement and Concrete Research 42 (2012) 972–981

Contents lists available at SciVerse ScienceDirect

Cement and Concrete Research

journal homepage: http://ees.elsevier.com/CEMCON/default.asp

Investigation of capillary flow in discrete cracks in cementitious materials

Diane Gardner *, Anthony Jefferson, Andrea Hoffman

Cardiff School of Engineering, Queen's Buildings, The Parade, Cardiff, CF24 3AA, UK

ARTICLE INFO

Article history:
Received 10 September 2011
Accepted 26 March 2012

Keywords:
Capillary flow
Transport properties (C)
Modelling (E)
Mortar (E)

ABSTRACT

A series of experimental studies are presented that simulate capillary flow of water in discrete cracks in cementitious materials. A number of amendments to existing capillary flow theory are adopted which take the form of correction parameters for stick–slip behaviour of the meniscus, frictional dissipation at the meniscus wall boundary and slip between the fluid and solid wall. A benchmark study to examine capillary flow in small diameter glass capillaries is reported and this provides data to validate the amended theoretical model. Predictions made using the amended model closely match the experimental results of capillary rise in discrete cracks in cementitious materials allowing the correction parameters for capillary flow in planar cracks to be determined. Finally, capillary rise in a discrete natural crack of known aperture is considered and a relationship is proposed which predicts the capillary rise response in a natural crack in terms of an equivalent planar crack.

1. Introduction and literature review

Expenditure on the repair and maintenance of civil infrastructure in developed countries now approaches 50% of their annual construction budget [1,2] and in 2009 the Federal Highway Administration in the USA stated that its transportation agencies would need $70.9 Billion alone to address the backlog of deficient bridges in the country [3]. The presence of pores and cracks in a cementitious matrix, the latter caused as a result of plastic shrinkage, structural loading and thermal effects amongst other actions, may lead to the promotion of deterioration processes such as freeze-thaw action, chloride ingress or carbonation and the independent or sometimes concurrent actions of these processes are partly responsible for reducing the service life of structures. This is of significant importance when considering the design and performance of critical civil infrastructure such as transportation links, water reservoirs, radioactive waste disposal facilities and confining enclosures of nuclear power plants [4,5].

Capillary absorption, driven primarily by surface tension, has been frequently noted in the literature [6–8] as one of the primary transport mechanisms by which aggressive agents from the environment ingress concrete. Conversely, capillary absorption also plays a role in the ability of a concrete to self-heal and recent work in the area of self-healing cementitious materials [9] has proved promising in enhancing the longevity of structures. The experimental modelling of capillary absorption of water in unsaturated concrete has been well documented by a number of researchers [10–12] and is generally measured using the sorptivity test [11,13,14]. In the absence of experimental data on the flow of water in discrete cracks in cementitious materials, researchers make reference to the flow of water in glass capillary tubes and between parallel plates of varying apertures [15–17]. However, these methods generally do not simulate explicitly the surface roughness and tortuosity of a discrete crack in a cementitious material, both of which have been considered by Collins and Sanjayan [7] to influence capillary absorption. Sielbold et al. [18] reported that in glass capillary tubes of known diameter the meniscus contact angle changed as a result of the velocity of the meniscus. Further work in this area by Hamraoui et al. [19] demonstrated that better agreement between experimental data and analytical solutions was achieved when this change in contact angle was taken into account.

Capillary absorption is usually described by the Lucas–Washburn (L–W) equation, derived by equating the capillary pressure difference across the interface between two immiscible fluids, to the pressure loss due to internal friction (the Hagen–Poiseuille equation).

A number of researchers have questioned the suitability of the L–W equation for long term capillary absorption studies [10,15,20,21]. However in the context of this paper it is capillary absorption in the short term (of the order of seconds) that is of interest. Numerical simulations and predictions of capillary absorption in cementitious materials have been presented by a number of researchers [8,12,19,21,22], although a far greater body of work is published on capillary flow in porous media in general [19,23–26] than on flow in discrete openings. Nevertheless, there has been some work which has considered such discrete flow behaviour. For example, fluid flow in a discrete crack in cementitious materials has been successfully modelled by Roels et al. [21] who used a moving front technique to track the movement of the meniscus through the

* Corresponding author at: School Office, Cardiff School of Engineering, Queen's Buildings, The Parade, Newport Road, Cardiff, CF24 3AA, UK. Tel.: +44 29 2087 0776; fax: +44 29 2087 4939.
E-mail addresses: gardnerdr@cf.ac.uk (D. Gardner), jeffersonad@cf.ac.uk (A. Jefferson), andihoffmanuk@aol.co.uk (A. Hoffman).

0008-8846/$ – see front matter © 2012 Elsevier Ltd. All rights reserved.
doi:10.1016/j.cemconres.2012.03.017

void space of a crack. This technique uses a combination of a quasi static pressure equation and a Darcian flux equation as presented by Karlsen et al. [27]. Essentially the same approach was used by Nitao and Buscheck [28] who adopted an adaptive time stepping scheme in their numerical solution of the governing flow equations.

The primary purpose of the paper is to present new experimental data on the capillary flow of water in discrete cracks in cementitious materials obtained via high speed video measurement. The paper also considers a mathematical model for capillary flow and uses flow in glass capillary tubes as a benchmark problem. The structure of the paper is as follows.

- Section 2 describes the theory of capillary flow and considers corrections to the well known Lucas–Washburn equation. Then, in the 2nd part of Section 2, corrections for flow prediction in capillary tubes are suggested by considering data from the literature as well as from new tests performed as part of the present study.
- Section 4 presents the new experimental data on fluid flow in openings in cementitious materials; including data from experiments with planar, four-stage sloped and natural apertures or 'cracks'.
- Section 5 provides comparisons between theoretical predictions, using the equations presented in Section 2, and the new experimental data, with appropriate correction coefficients being suggested. Finally, in Section 5, a study is described which ascertains whether the flow behaviour in a natural crack can be adequately described by that in a planar aperture of equivalent opening.

The present investigation concentrates on flow in a discrete crack with no consideration being given to flow into or out of the porous media adjacent to the discrete opening. The importance of including both aspects of flow behaviour when simulating these problems with, for example, a finite element model, is however fully acknowledged [29].

2. Theoretical background

The L–W equation, describes the dynamic flow of liquid in a capillary tube (see Fig. 1), and employs a force balance between a driving capillary force and a retarding viscous force [30]. To complete the momentum balance, it is necessary to include gravitational and inertial terms, as shown in Eq. (1) [26].

$$2\pi r\gamma\cos(\theta)-\pi r^2\rho g z\sin(\phi)-8\pi\mu z\dot{z}-\rho\pi r^2\frac{\partial}{\partial t}(z\dot{z})=0 \tag{1}$$

in which z = capillary rise height (m), γ = surface tension (N/m), θ = liquid/solid contact angle (°), ϕ = tube inclination angle (°); ρ is the density of liquid (kg/m^3), g = gravitational acceleration (m/s^2), r = radius of the capillary (m), μ = dynamic viscosity (Ns/m^2), t = capillary rise time (s).

The inertial term, as demonstrated by Quéré [30], Lorenceau et al. [31] and Bosanquet [32], can be important during the initial stages of capillary rise. Hamraoui and Nylander [26], Martic et al. [33] and Xue et al. [34] along with a number of other investigators have neglected the inertial term in their calculations when considering small diameter capillary tubes. Fries and Dreyer [35] provide an estimate of the relative rise height after which the inertial term may be ignored. For a capillary diameter of 0.3 mm, this relative rise height is 15% of the maximum rise height and at this height the deviation from a solution that includes inertia is 3%, with the error gradually reducing beyond this point. It is therefore proposed that the inertial term is neglected in the development of the theoretical capillary rise response model in this paper, since it can be considered negligible in the timescales and anticipated rise heights of the flow simulations performed.

Rearranging Eq. (1) and neglecting the inertial term, as previously discussed, gives the following form of the L–W equation:

$$p_c-\rho g z\sin(\phi)-\frac{\mu}{k}z\dot{z}=0 \tag{2}$$

in which the effective permeability term $k=r^2/8$ [23]

The capillary pressure term in Eq. (2) is given by Eq. (3), which is often named the Young–Laplace equation [21]:

$$p_c=\frac{2\gamma\cos(\theta)}{r} \tag{3}$$

at static equilibrium:

$$h_{eq}=\frac{p_c}{\rho g\sin(\phi)} \tag{4}$$

where h_{eq} is the equilibrium height where the hydrostatic pressure balances the capillary pressure.

To allow for the change in fluid velocity as a result of non-uniform capillaries Young [23] modified Eq. (2) to the following form:

$$\eta\dot{z}=(p_c-\rho g z\sin(\phi)) \tag{5}$$

which was derived by applying the following mass conservation equation :

$$\dot{z}A(z)=v(x)A(x) \tag{6}$$

and in which

$$\eta=\mu A(z)\int_0^z\frac{1}{k}\frac{1}{A(x)}dx. \tag{7}$$

It is noted that the term η represents the total viscous resistance to flow (per unit area at the meniscus) and has the units Ns/m^3.

Eq. (7) is solved using a direct integration time-stepping procedure. A check is undertaken to ensure that the time step is sufficiently small to give converged results.

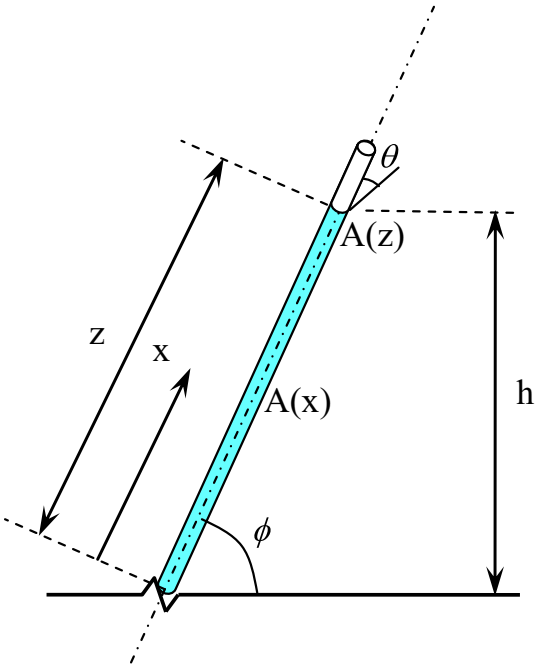

Fig. 1. Illustration of the parameters used to model water flow in a uniform capillary.

A similar numerical solution has been developed here for planar cracks, whereby the radius of the capillary tube, r, is replaced by the crack width, b and the effective permeability term takes the value $k = b^2/12$ [36].

In the present benchmark experiments it was found that neither the shape nor the final rise height matched the response of the standard form of the L–W equation. Other authors have also found discrepancies with this theory and a number of corrections have been proposed. These corrections have sought to address (i) pinning (or stick–slip) behaviour at the meniscus [37] (ii) velocity-dependent dynamic contact angle [33], which Hamraoui and Nylander [26] also suggest is related to frictional dissipation at the meniscus-wall boundary and (iii) general slip between the fluid and solid wall, which was considered in a classical solution by Mooney [38] (see Kemerker and Edwards [39]). These corrections are explored more fully below.

(i) Schäffer and Wong [37] give the following expression for the 'threshold pinning pressure' (or stick–slip) for a vertical capillary tube,

$$p_s = \rho g\left(h_{eq} - h_s\right) \tag{8}$$

in which h_s is the rise height allowing for pinning.
p_s may be treated as an effective reduction in capillary pressure such that the effective capillary pressure becomes $p_{ceff} = p_c - p_s$

Hence, the resulting correction to allow for pinning may be expressed as:

$$p_{ceff} = p_c - p_s = p_c(1-\beta_s) \tag{9}$$

in which

$$\beta_s = 1 - \frac{h_s}{h_{eq}} \tag{10}$$

(ii) Hamraoui and Nylander [26] propose a correction in the form of a retardation constant to allow for frictional dissipation at the moving front. They suggest that the principle source of such losses may be related to the dynamic contact angle [40] and give the following expression for the dynamic contact angle:

$$\gamma\cos(\theta(t)) = \gamma\cos(\theta_0) - \beta_m\dot{z} \tag{11}$$

in which θ_0 = static contact angle and β_m should be constant for a given system. Blake [40] gives the following expression for β_m, although the difficulty in determining λ means that the β_m is here treated as a material constant (with units Ns/m^2) to be determined from experimental data.

$$\beta_m = \frac{k_B T \nu}{2\pi\lambda^3 \kappa_0^s \hbar}\eta \tag{12}$$

here, λ is the distance between adsorption sites on the solid surface, κ_0^s is the surface rate constant for molecular displacements, ν is the molecular volume of the liquid, k_B and $2\pi\hbar$ are the Boltzmann and Planck constants, respectively, T is the temperature and η the viscosity of the liquid.

(iii) A well-established correction for wall slip was given many years ago by Mooney [38] which in effect modifies the Hagen–Poiseuille (H–P) equation. For a capillary tube the Mooney's modified H–P equation may be expressed as follows:

$$\dot{z} = \left(\frac{r\beta_w}{2} + \frac{r^2}{8\mu}\right)\left(\frac{dp}{dx}\right) \tag{13}$$

in which p(x) is the mean pressure at position x along the tube. Mooney's constant β_w has the units m^3/Ns and it is noted that dp/dx is replaced by p_c/z in the present form of the L–W equation.

Including all three of these terms in Eq. (2), and again neglecting the inertial term, gives the amended L–W equation as follows:

$$p_{c0}(1-\beta_s) - \frac{2\beta_m\dot{z}}{r} - \rho g z\sin(\phi) - \left(\frac{z}{\frac{r\beta_w}{2} + \frac{r^2}{8\mu}}\right)\dot{z} = 0 \tag{14}$$

in which the superior dot denotes the time derivative

$$\text{noting that } p_{c0} = \frac{2\gamma\cos(\theta_0)}{r}. \tag{15}$$

It may be seen that the pinning correction was applied only to p_{c0}. Rearranging Eq. (14) gives:

$$\dot{z} = \frac{p_{c0}(1-\beta_s) - \rho g z\sin(\phi)}{\frac{2\beta_m}{r} + \left(\frac{z}{\frac{r\beta_w}{2} + \frac{r^2}{8\mu}}\right)}. \tag{16}$$

In order to explore the effect of each term on a generalised response, the capillary flow of water predicted by Eq. (16), in two different glass capillary tubes of 0.3 mm and 1.0 mm diameter, is compared to that predicted by the standard L–W equation.

The standard L–W response was obtained by the numerical integration of Eq. (16) with all beta factors set to zero. However, the numerical response, thus calculated, was checked against the analytical expression given by Fries and Dreyer [41], with the results from the two calculations being the same to within the precision of the calculation and thus indistinguishable from each other on graphs in Fig. 2.

The results are normalised by considering h_{eq}, the equilibrium rise height as obtained by balancing the capillary force with the weight of the liquid column (Eqs. (3) and (4)), and t^*, the time taken to reach 99% of h_{eq}. The dimensionless time parameter (t/t^*) for the L–W analytical solution has been used as the abscissa in each simulation to provide a guide on how each correction modified the response curve effectively in real time. It should be noted that all simulations, with the exception of those which had a non-zero β_s correction factor, reached the limiting h_{eq}, for the experimental arrangement simulated.

As would be expected from Eq. (14), it may be seen in Fig. 2 that an increase in β_s causes a decrease in both the final rise height h_{eq} and the rise rate. It can also be observed that the inclusion of the β_m correction factor retards the capillary rise response and that an increase in the β_w correction accelerates the capillary rise response of the system as a result of the decreased net resistance to flow.

The main purpose of including the comparison in Fig. 2 is to show the relative effect of each parameter on the characteristic capillary rise response and thereby provide guidance for the corrections required for the prediction of the fluid rise response in cracks in cementitious materials, which are considered below.

Experimental validation of the three corrections proposed was performed in the first instance using capillary rise data recorded by LeGrande and Rense [42] for water and ethyl in chemically cleaned and wetted glass capillary tubes of known internal diameter. Good agreement between the experimental data and the amended L–W equation proposed in Eq. (16) is observed for a capillary diameter of 0.570 mm, as shown in Fig. 3 where β_s, β_m and β_w take the values of 0.01, 0.22 Ns/m^2 and 0 m^3/Ns and 0.01, 0.07 Ns/m^2 and 0 m^3/Ns for

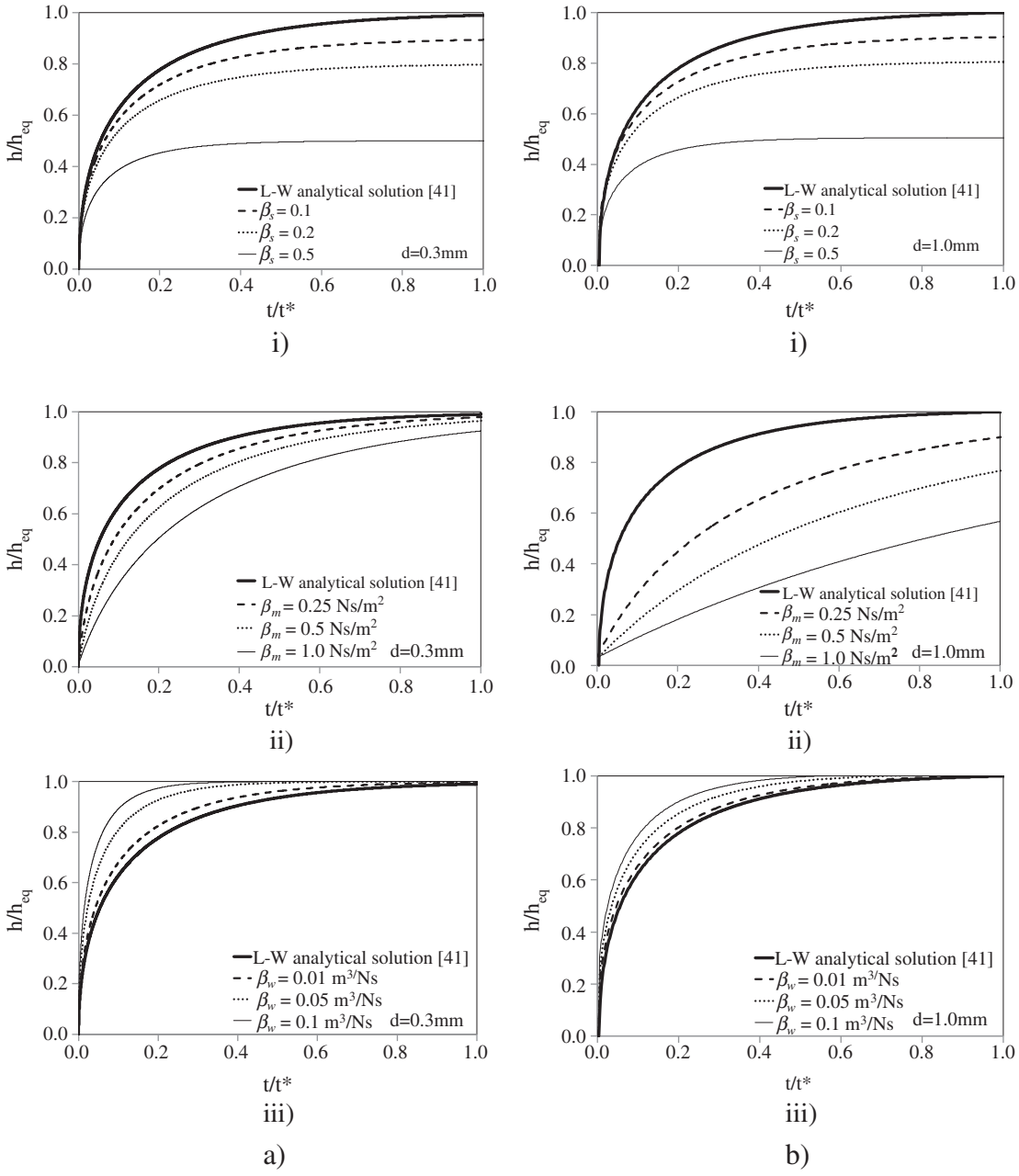

Fig. 2. Effect of correction parameters i) β_s, ii) β_m and iii) β_w on the capillary rise response of a) water in a glass capillary of diameter 0.30 mm b) water in a glass capillary of diameter 1.0 mm.

water and ethyl respectively. Also presented in Fig. 3 is the rate of capillary rise calculated using the analytical solution to the L–W equation from [41].

Experimental validations were also performed as part of this study using borosilicate glass tubes supplied by CM Scientific Ltd. These tubes were used in a nominally 'as supplied' clean condition but were not subjected to any additional cleaning or wetting prior to testing. Capillary tubes of 0.2 mm, 0.5 mm and 1.0 mm diameter were tested.

The actual capillary rise height for all three capillary diameters was below that predicted by the standard form of the L–W equation, even after dimensional tolerances of the capillary tubes were considered. The full capillary rise response for these capillary tubes can be seen in Fig. 4. For the experiments conducted, the correction factors required to provide a close match with the experimental data were values of 0.35 for β_s, 0.35 Ns/m^2 for β_m and 0 m^3/Ns for β_w. In contrast to the correction parameters used to simulate the experiments of LeGrande and Rense [42], the magnitude of the factors used here suggest a greater degree of contamination and roughness in comparison with the capillary tubes used by LeGrande and Rense.

3. Experimental details

3.1. Materials and mix proportions

A mortar, with an average compressive strength of 36.7 N/mm^2, was used throughout the study. Cement type CEM IV/B-V 32,5R conforming to BS EN 197-1:2000, together with a marine dredged sand, with maximum particle size of 2 mm, were employed in the mix in the following proportions 540 kg/m^3:1618 kg/m^3:242 kg/m^3 (cement:sand:water).

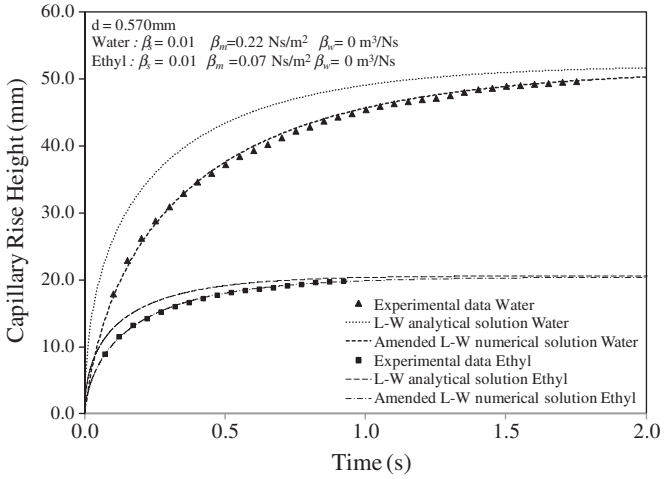

Fig. 3. Validation of theoretical model with published data [42] for d = 0.570 mm.

3.2. Specimen preparation

The experimental studies were performed on mortar specimens after 7 days and 28 days of curing. In the former, the specimens were demoulded and left to air cure until the testing date. In the latter, the specimens were demoulded and the prisms were wrapped in damp hessian for 14 days and then left to air cure at a temperature of 21 °C for a further 14 days. Prisms of size 75 mm × 75 mm × 255 mm were cast and planar (P) (Fig. 5(a)) and four-stage sloped (FSS) (Fig. 5(b)) openings (or equivalent 'cracks') were formed by wet cutting each prism into seven pairs of 30 mm × 30 mm × 75 mm specimens using a circular saw. The specimens were then left to dry in the laboratory environment for a further week prior to testing. A number of specimens were tested in a saturated condition, which entailed saturating the specimens for 48 h before testing. Four-stage sloped cracks were formed using a series of folded plates of 2 mm thickness placed vertically in the prismatic moulds, before being cut in the same manner as the planar crack specimens. These plates were manufactured so that the angle of the flow path deviated from the vertical by ±5°. Both planar and four-stage sloped crack surfaces were filed with a fine glass paper and cleaned with pressurised air prior to testing. A natural crack configuration (N), as demonstrated in Fig. 5(c), was formed by loading a 75 mm × 75 mm × 255 mm centrally notched specimen in three point bending until failure. Two 75 mm × 75 mm × 25 mm specimens were subsequently cut from the crack zone as indicated in Fig. 6. Pressurised air was blown over the natural crack faces to remove any loose fragments.

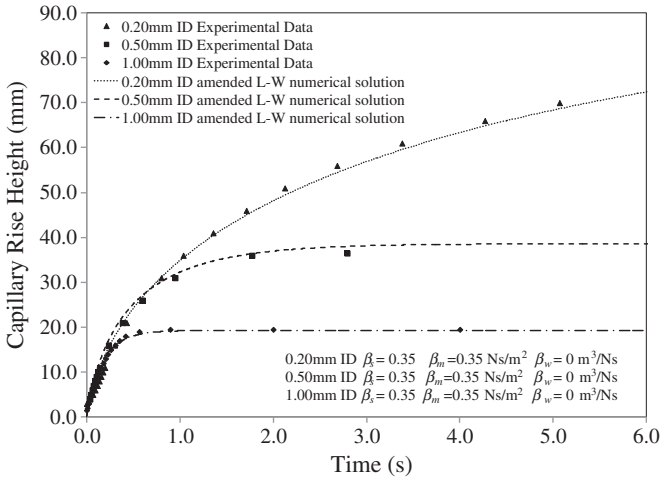

Fig. 4. Comparison of experimental data and numerical model for borosilicate glass tubes.

For each crack type, a series of crack apertures were achieved by using spacers which comprised short lengths of steel, nickel or tin wires with diameters varying from 0.094 to 1.170 mm. The wire was placed between a pair of mortar specimens and the pair of specimens clamped together, as shown schematically in Fig. 5(a) to (c). A series of measurements of the crack aperture at the surface were taken using a Beck Luminex microscope and a mean crack aperture was calculated based on these observations. The mean crack aperture serves as one of the specimen references throughout the experimental and numerical simulations. All experiments were performed in triplicate and specimen testing designations were "crack configuration_aperture (mm)_age (days)", for example P_0.344_28 represents a planar crack of 0.344 mm mean aperture and an age of 28 days.

3.3. Capillary flow simulations

Specimens were weighed and their weight was recorded. These data were recorded to allow the moisture content of each specimen to be calculated. The clamped specimens were then placed on top of two small blocks in a shallow tray such that the base of the specimens was 1.38 mm above the base of the tray. The capillary rise was captured with a high speed MOTIONeer camera, as manufactured by AOS technologies. Such equipment has been successfully used for motion analysis of body parts in the medical profession. A recording speed of 250 frames per second was selected in order to obtain images of sufficient clarity and frequency for data processing purposes. The camera was mounted on a platform 300 mm in front of the specimens. The experimental set up is shown in Fig. 7. A laminated scale was used to measure capillary rise and was adhered to one side of the crack on the front face of the specimens. During the experiment adjustable high intensity lighting was used in front of and behind the specimens to enhance the visibility of the crack, and this was only switched on during the recording sequence to ensure a negligible change in water temperature and viscosity during the test. Due to the tortuosity of the cracks in the natural crack configuration, there was difficulty in illuminating the crack using the existing lighting and therefore fluorescein was added to the water and the experiment was conducted in a darkened cabinet under an Ultra-Violet (UV) light. The effect of using fluorescein in the water was checked in a series of tests in capillary tubes, in which the addition of fluorescein to water in concentrations of 0.01% and 0.1% resulted in negligible variations in the equilibrium rise height and capillary rise response. On commencement of the recording, 50 ml of distilled water at room temperature (21 °C) was added to the tray. Experiments ceased after no further capillary rise was observed or the capillary rise reached the full height of the specimens.

4. Experimental results

The results presented examine the effect of crack aperture, specimen age, degree of saturation and crack configuration on the level and rate of capillary rise height. Capillary rise heights were extracted from the video files, in a similar sequence to that illustrated in Fig. 8 which shows a typical capillary rise height sequence for a planar crack aperture of 0.502 mm. The values shown in Fig. 8 and represented in the results have been corrected to represent the capillary rise above the free water surface.

Capillary rise heights for a range of crack apertures for a planar crack configuration are shown in Fig. 9. The specimens under examination were in the laboratory dry state. It is apparent that for planar crack apertures greater than 0.237 mm the equilibrium capillary rise height is equal to that predicted from capillary flow theory, using Eqs. (3) and (4) and assuming an equilibrium contact angle of zero and surface tension of water of 0.0728 N/m. Similarly for the four-stage sloped cracks, the equilibrium rise height, relative to the crack aperture, was achieved regardless of crack inclination.

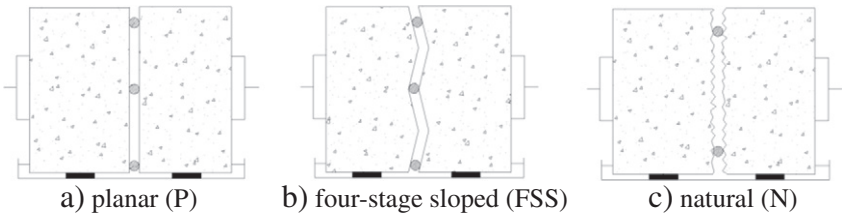

Fig. 5. Schematic representation of crack configurations.

The capillary rise data for 3 different crack configurations for 3 different apertures is given in Fig. 10. The data clearly show the reduction in rise height as the crack aperture increases when considering each of the 3 crack configurations. More importantly is it evident that whilst there is generally good agreement between the planar and four-stage sloped crack configuration at the same crack aperture, the capillary rise height for the natural crack configuration at all apertures is lower. The natural crack aperture varies throughout and the tortuous nature of these crack surfaces suggests a longer flow path when the height of the asperities is greater than or equal to the crack opening, which is the case in the present examples.

However, it is apparent that it may be possible to establish an equivalent planar crack aperture for a natural crack configuration of known aperture and this is explored further when the experimental results of the planar crack configuration are numerically modelled.

Fig. 11 presents the effect of specimen age on the rate of capillary rise height. The equilibrium rise heights for each crack aperture are the same regardless of the age of the specimen yet the rates of capillary rise are markedly less for the 28 day specimens. This could be related to the effect of the time dependent development of the mortar microstructure on the dynamic resistive forces acting during capillary flow.

When considering the effect of specimen saturation on capillary rise height, as presented in Fig. 12, it can be seen that although the capillary rise tends towards the 'dry' rise height, the rate of capillary rise is slower for saturated specimens. For a porous material, the presence of water in the pores adjacent to a discrete crack would probably disrupt the development of attractive forces at the meniscus wall interface and thereby result in a reduced capillary driving force.

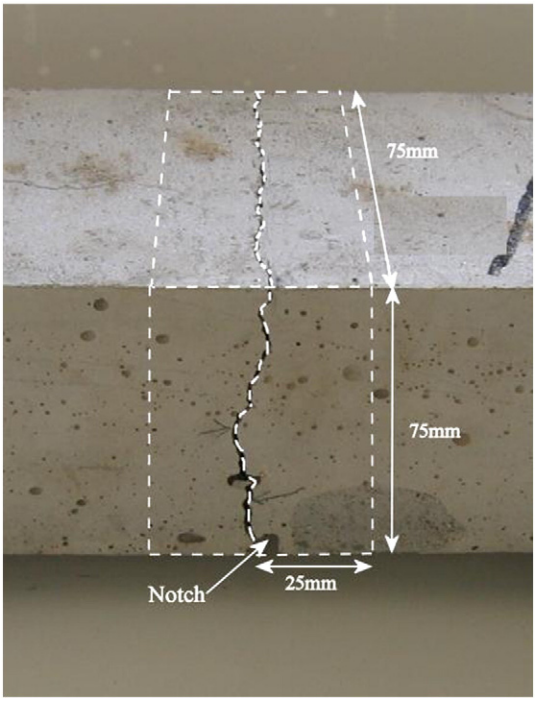

Fig. 6. Manufacture of natural crack configuration.

5. Comparison of numerical and experimental results for planar and natural crack configurations

In this section, comparisons are made between the results from experiments described in Section 4 of this paper and the results obtained from the amended L–W equation derived in Section 2. Experimental data from additional planar crack configuration tests were also used to further validate the numerical model based on the amended L–W equation. Fig. 13 presents the capillary rise response in planar cracks and the β_s, β_m and β_w correction factors that were used to simulate the experimental data.

In order to numerically model the capillary rise response for a planar crack aperture the mean crack aperture measured in the experiment was used to predict the theoretical equilibrium rise height. On obtaining this, the β_s correction parameter was adjusted until the experimental rise height was achieved. The correction parameters β_m and β_w were then modified until the capillary rise response as observed in the experiment was reproduced. It can be concluded from the good agreement between the experimental and numerical results that for a planar crack in an unsaturated mortar material β_s takes the value of 0.01. The correction parameter β_m assumes the value of 0.55 Ns/m^2 for all crack apertures tested and this reflects the standardised surface roughness that was achieved in the specimen preparation prior to testing, confirming Blake's theory [40] that this correction parameter is constant for any particular combination of material and fluid considered. The β_w correction factor is 0 m^3/Ns in all cases, indicating no significant effect of wall slip on the capillary rise response of water in planar cracks in a cementitious material.

One of the main aims of this research was to establish an equivalent planar crack capillary rise response for water flow in a natural crack of known aperture. Two methods were considered for this. The first method concerned the adjustment of the correction parameters proposed in this study, in particular the β_s parameter which one would expect to be different for a rough surface, whilst using the actual mean crack aperture as measured in the experiments. The second method involved choosing correction parameters consistent with those of a planar crack and an equivalent mean crack aperture that would give the same capillary rise response as that of a natural crack of known aperture. Trials suggested that the second method produced more consistent predictions than the first method and therefore this approach was followed. Fig. 14 shows the capillary rise responses for an equivalent planar crack compared to the experimental natural crack configuration. The correction parameters used are those which relate to the planar equivalent aperture. There is a close match between the numerical and experimental capillary rise responses for the 0.170 to 0.502 mm crack apertures. The agreement is not as close for the 0.620 mm case as for the other openings but it is observed that the shape of the experimental capillary rise response for the 0.620 mm crack aperture does not follow the 'standard' form. This may have been caused by the presence of discrete particles wedged in the crack but the reason for this difference is left as an open question.

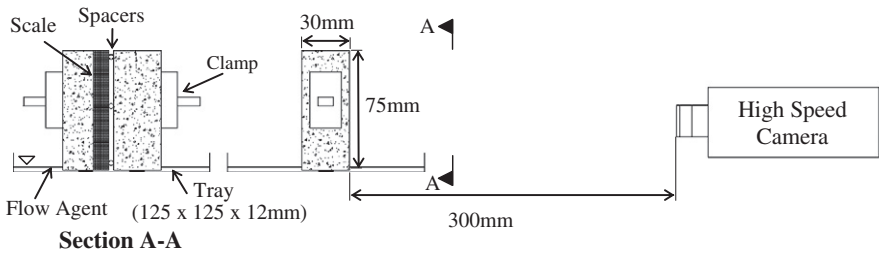

Fig. 7. Experimental arrangement for capillary flow simulations.

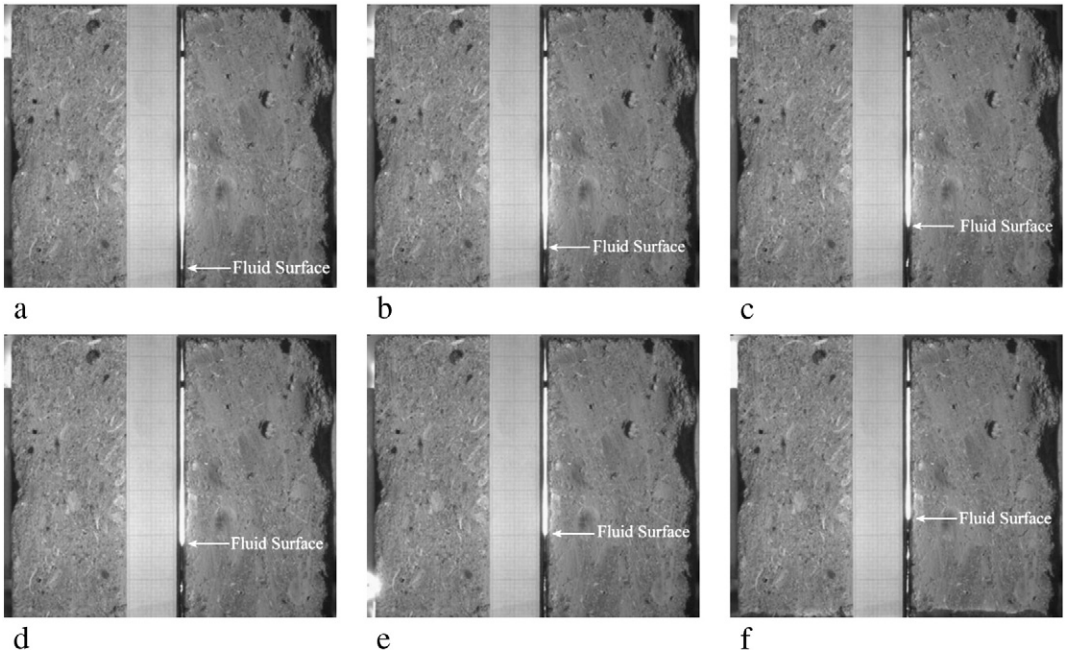

Fig. 8. Capillary rise height with time for P_0.502_28 a) 13.18 mm at 0.024 s; b) 18.18 mm at 0.100 s; c) 23.18 mm at 0.260 s; d) 25.68 mm at 0.381 s; e) 28.18 mm at 0.764 s; and f) 31.18 mm at 1.664 s

The computed effective planar crack openings are plotted against the corresponding actual measured rough crack openings in Fig. 15. It would seem reasonable to assume that, as the natural crack aperture increases, the capillary rise response would tend towards that of a planar crack of equal aperture since the relative roughness of natural crack surfaces reduces in proportion to the opening as the aperture increases. The opening beyond which the difference between the effective planar opening and the rough crack opening has a negligible effect on the computed capillary rise response is denoted c_{w_e}.

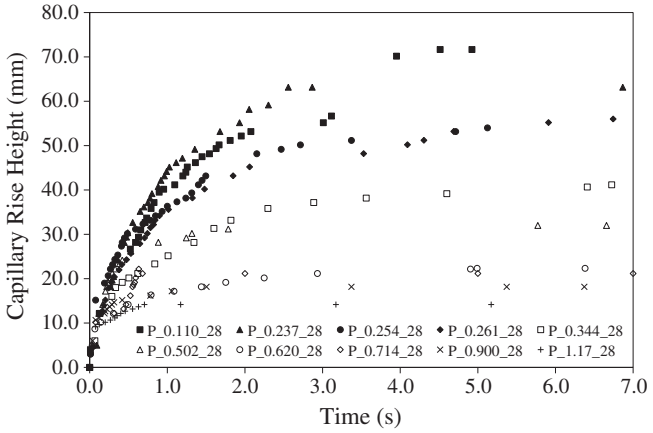

Fig. 9. Capillary rise height data for planar crack configuration.

It is expected that the value of c_{w_e} would be dependent on the roughness of the crack surface which in turn would be a function of the maximum particle size in the cementitious matrix. As shown in Fig. 15, measurements of h_{eq} for natural crack apertures of 2 mm and 3 mm were shown to be within 1% of the values of h_{eq} for planar cracks predicted by Eq. (4). This suggests that a crack opening of 2 mm is a reasonable limit beyond which it may be assumed that the behaviour of natural and planar cracks is indistinguishable, for the present material.

Finally, we tentatively propose a relationship, given in Eq. (17), to predict the equivalent planar crack opening in terms of the actual mean rough crack opening. It is recognised that further investigations, using a larger range of crack openings and concrete mixes with different maximum aggregate sizes, would be needed to fully validate the proposed expression.

$$c_{w_p} = k(\zeta) c_{w_n} \tag{17}$$

where

$$k(\zeta) = \zeta k_0 + (1-\zeta) k_m$$

and

$$\zeta = \left(1 - \frac{c_{w_n}}{c_{w_e}}\right)^n$$

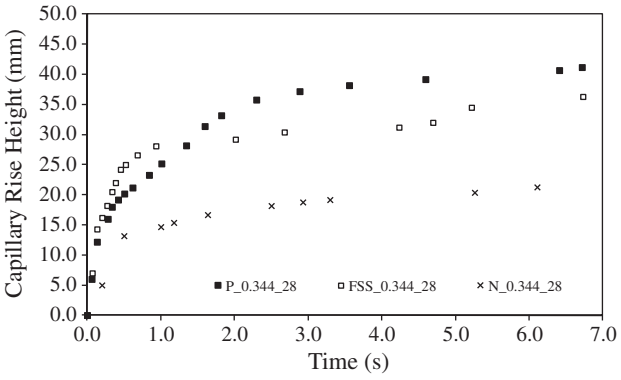

(a) 0.344mm aperture

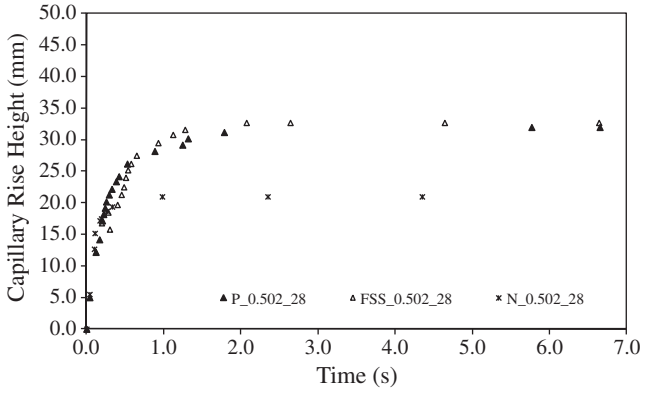

(b) 0.502mm aperture

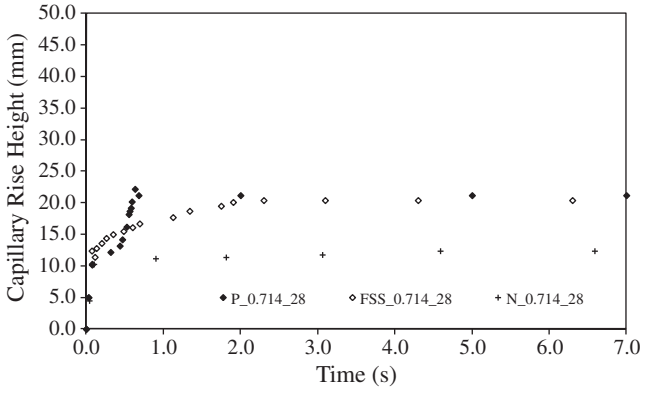

(c) 0.714mm aperture

Fig. 10. Comparison of capillary rise height data for different crack configurations for three crack apertures. (a) 0.344 mm (b) 0.502 mm (c) 0.714 mm.

in which k_0 is the gradient of the initial slope of the graph and k_m is the gradient of the graph as it becomes asymptotic to the crack convergence value. The closest match to the experimental data was found when $n=6$, $k_0=4$, $k_m=1$ and as discussed previously $c_{w_e}=2$ mm.

6. Conclusions

The experimental modelling of capillary flow of water in cementitious materials is generally considered in the context of flow through a porous continuum and as a result there is little published data available on flow in discrete cracks in concrete or mortar.

The experimental arrangement used in this study allowed capillary rise response of water in a range of crack configurations to be measured. Planar, four-stage sloped and natural crack configurations were all considered as well as the effect of specimen age and saturation on the shape and height of the capillary rise response. It was apparent that 7 day specimens had a faster capillary rise response than 28 day specimens although the equilibrium rise heights for each tended towards the same value. Similarly, unsaturated specimens had faster capillary rise response than saturated specimens and it is suggested that this may be due to an interaction, in terms of attractive forces between the water in the capillary and the water on the wetted surface that may retard the rate of capillary rise. Natural cracks had the lowest rise heights of the three

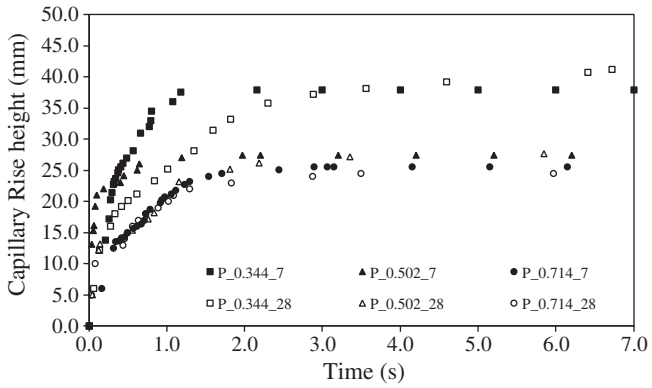

Fig. 11. Rate of capillary rise height in 7 day and 28 day old specimens.

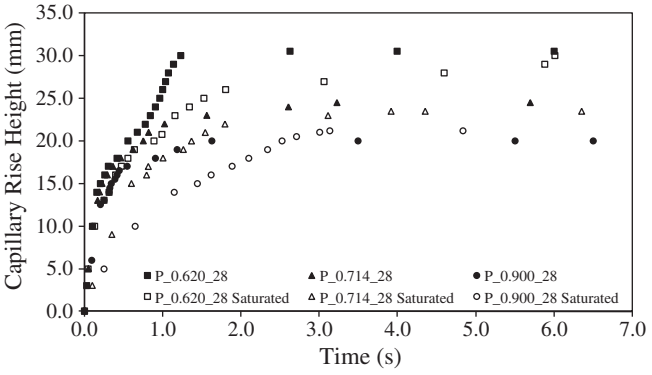

Fig. 12. Rate of capillary rise for saturated and unsaturated specimens.

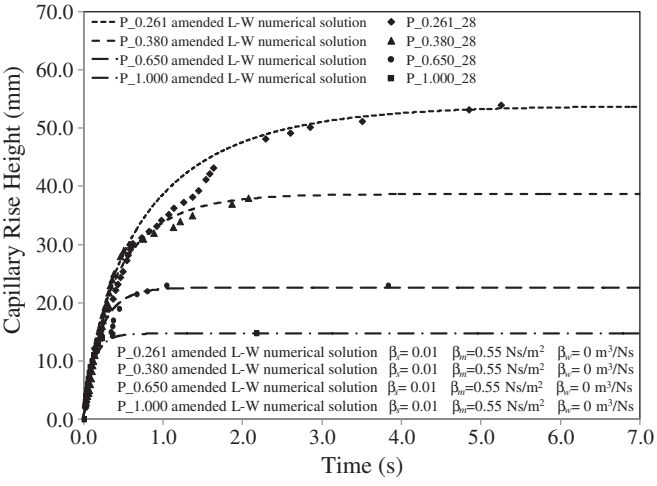

Fig. 13. Comparison of experimental data to amended L–W numerical solution for a range of planar crack apertures.

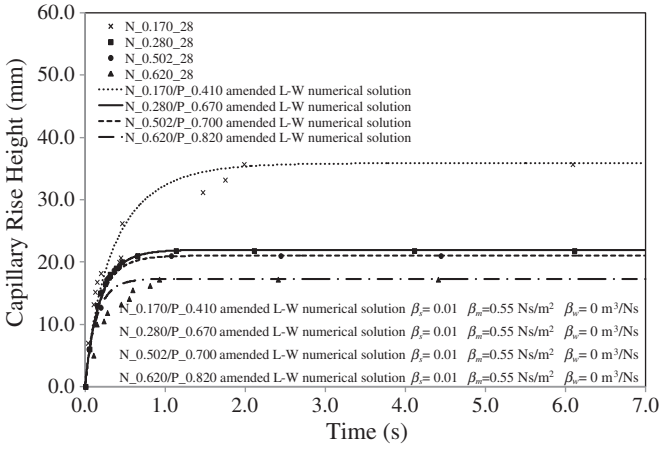

Fig. 14. Comparison of experimental data to amended L–W numerical solution for a range of natural cracks with equivalent planar apertures.

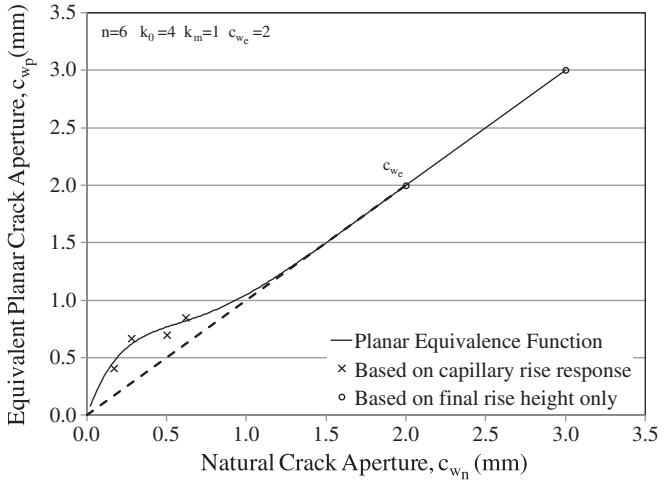

Fig. 15. Planar equivalence function for capillary flow in natural cracks of known aperture.

configurations considered, although this is not unexpected due to the increased roughness of the crack surface and three dimensional nature of the crack plane.

Although equilibrium capillary rise heights in agreement with the Young–Laplace equation were observed for the planar and four-stage sloped crack configurations, the shape of the capillary rise response was different from that predicted by the standard L–W equation. Therefore, three correction factors, similar to those presented by others in the literature, were adopted. The benchmark study demonstrated that for glass capillary tubes of known diameter the correction parameters are strongly influenced by the treatment of capillary tubes prior to testing, such as the removal of contaminants. For the capillary flow of water in discrete cracks in a mortar with maximum aggregate size of 2 mm the correction parameters for stick–slip and frictional dissipation at the meniscus wall (β_s and β_m) take the values of 0.01 and 0.55 Ns/m^2 respectively whilst the parameter incorporating the slip between the fluid and solid wall (β_w) was 0 m^3/Ns in all cases showing no significant influence of wall slip on the capillary rise response.

More importantly it has been shown that it is possible to establish a relationship that will give the capillary rise response for a natural crack of known aperture by using an equivalent planar crack aperture. Such a relationship is currently only valid for unsaturated flow of water in discrete cracks in mortar, although it should be possible to develop this further to consider the flow of other liquids in discrete cracks in concrete.

References

[1] E. Cailleux, V. Pollet, Investigations on the development of self-healing properties in protective coatings for concrete and repair mortars, Proceedings of the Second International Conference on Self-healing Materials, Chicago USA, 2009, p. 120.
[2] Corporatewatch, The construction sector: a brief overviewSee, http://www.corporatewatch.org/?lid=262for further details. Accessed 04/06/2011.
[3] United States Department of Transportation — Federal Highway Administration, SAFETEA-LU Funding Tables, 2009, p. 23. See http://www.fhwa.dot.gov/safetealu/fundtables.htm. (File: revfy09comptables.pdf). Accessed 05/09/2011.
[4] P. Picandet, A. Khelidj, H. Bellegou, Crack effects on gas and water permeability of concretes, Cem. Concr. Res. 39 (6) (2009) 537–547.
[5] C. Joseph, A.D. Jefferson, B. Isaacs, R.J. Lark, Experimental investigation of adhesive-based self-healing of cementitious materials, Mag. Concr. Res. 62 (11) (2010) 831–843.
[6] M.D. Lepech, V.C. Li, Water permeability of engineered cementitious composites, Cem. Concr. Compos. 31 (10) (2009) 744–753.
[7] F. Collins, J. Sanjayan, Unsaturated capillary flow within alkali activated slag concrete, J. Mater. Civ. Eng. 20 (9) (2008) 565–570.
[8] L. Hanžič, R. Ilič, Relationship between liquid sorptivity and capillarity in concrete, Cem. Concr. Res. 33 (9) (2003) 1385–1388.
[9] C. Joseph, D. Gardner, A. Jefferson, R. Lark, B. Isaacs, Self healing cementitious materials: a review of recent work, Proc. Inst. Civ. Eng. Constr. Mater. 164 (1) (2010) 29–41.
[10] L. Hanžič, L. Kosec, I. Anžel, Capillary absorption in concrete and the Lucas–Washburn equation, Cem. Concr. Compos. 32 (1) (2010) 84–91.
[11] N.S. Martys, C.E. Ferraris, Capillary transport in mortars and concrete, Cem. Concr. Res. 27 (5) (1997) 747–760.
[12] A. Razak, H.K. Chai, H.S. Wong, Near surface characteristics of concrete containing supplementary cementing materials, Cem. Concr. Compos. 26 (2004) 883–889.
[13] C. Hall, W.D. Hoff, Water Transport in Brick, Stone and Concrete, 1st edition Taylor & Francis, 2002.
[14] M.C. Torrijos, G. Giaccio, Z. Zerbino, Internal cracking and transport properties in damaged concretes, Mater. Struct. 43 (2010) 109–121.
[15] D.A. Lockington, J.Y. Parlange, A new equation for macroscopic description of capillary rise in porous media, J. Colloid Interface Sci. 278 (2) (2004) 404–409.
[16] B.V. Zhmud, F. Tiberg, K. Hallstensson, Dynamics of capillary rise, J. Colloid Interface Sci. 228 (2000) 263–269.
[17] J.W. Bullard, E. Garboczi, Capillary rise between planar surfaces, Phys. Rev. E 79 (1) (2009) 1–8.
[18] A. Siebold, M. Nardin, J. Schultz, A. Walliser, M. Oppliger, Effect of dynamic contact angle on capillary rise phenomena, Colloids Surf. A 161 (2000) 81–87.
[19] A. Hamraoui, K. Thuresson, T. Nylander, V. Yaminsky, Can a dynamic contact angle be understood in terms of a friction coefficient? J. Colloid Interface Sci. 226 (2000) 199–204.
[20] M. Lago, M. Araujo, Capillary rise in porous media, J. Colloid Interface Sci. 234 (1) (2001) 35–43.
[21] C. Hall, Water movement in porous building materials—I. Unsaturated flow theory and its applications, Build. Environ. 12 (2) (1977) 117–125.
[22] S. Roels, K. Vandersteen, J. Carmeliet, Measuring and simulating moisture uptake in a fractured porous medium, Adv. Water Resour. 26 (2003) 237–246.
[23] W.-B. Young, Analysis of capillary flows in non-uniform cross-sectional capillaries, Colloids Surf. A 234 (2004) 123–128.
[24] T. Metzger, E. Tsotsas, Network models for capillary porous media: application to drying technology, Chem. Ing. Tech. 82 (6) (2010) 869–879.
[25] B. Markicevic, H.K. Navaz, Numerical solution of wetting fluid spread into porous media, Int. J. Numer. Methods Heat Fluid Flow 19 (3/4) (2008) 521–534.
[26] A. Hamraoui, T. Nylander, Analytical approach for the Lucas–Washburn equation, J. Colloid Interface Sci. 250 (2) (2002) 415–421.
[27] K.H. Karlsen, K.A. Lie, N.H. Risebro, J. Froyen, A front tracking approach to a two-phase fluid flow model with capillary forces, In Situ 22 (1) (1998) 59–89.
[28] J.J. Nitao, T.A. Buscheck, Infiltration of a liquid front in an unsaturated, fractured porous-medium, Water Resour. Res. 27 (8) (1991) 2099–2112.
[29] J. Rethore, R. de Borst, M.A. Abellan, A two-scale model for fluid flow in an unsaturated porous medium with cohesive cracks, Comput. Mech. 42 (2008) 227–238.
[30] D. Quéré, Inertial capillarity, Europhys. Lett. 39 (5) (1997) 533–538.
[31] É. Lorenceau, D. Quéré, J.-Y. Ollitrault, C. Clanet, Gravitational oscillations of a liquid column in a pipe, Phys. Fluids 14 (6) (2002) 1985–1992.
[32] C.H. Bosanquet, On the flow of liquids into capillary tubes, Philos. Mag. Ser. 6 (1923) 525–531.
[33] G. Martic, J. Coninck, T.D. Blake, Influence of the dynamic contact angle on the characterization of porous media, J. Colloid Interface Sci. 263 (2003) 213–216.
[34] H.T. Xue, Z.N. Fang, Y. Yang, J.P. Huang, L.W. Zhou, Contact angle determined by spontaneous dynamic capillary rises with hydrostatic effects: experiment and theory, Chem. Phys. Lett. 432 (2006) 326–330.
[35] N. Fries, M. Dreyer, The transition from inertial to viscous flow in capillary rise, J. Colloid Interface Sci. 327 (1) (2008) 125–128.

[36] R.W. Zimmerman, D. Chen, N.G.W. Cook, The effect of contact area on the permeability of fractures, J. Hydrol. 139 (1992) 79–96.
[37] E. Schäffer, P. Wong, Dynamics of contact line pinning in capillary rise and fall, Phys. Rev. Lett. 80 (14) (1998) 3069–3072.
[38] M. Mooney, Explicit formulations for slip and fluidity, J. Rheol. 2 (1931) 210–222.
[39] P.A. Kemerker, B.J. Edwards, An experimental study of slip flow in capillaries and semihyperbolically converging dies, Polym. Eng. Sci. 47 (2) (2007) 159–167.
[40] T.D. Blake, in: J.C. Berg (Ed.), Wettability, Marcel Dekker, New York, 1993.
[41] N. Fries, M. Dreyer, An analytic solution of capillary rise restrained by gravity, J. Colloid Interface Sci. 320 (2008) 259–263.
[42] E. Legrande, W. Rense, Data on rate of capillary rise, J. Appl. Phys. 16 (1945) 843–846.